

Catalysis Science & Technology

Accepted Manuscript



This is an *Accepted Manuscript*, which has been through the Royal Society of Chemistry peer review process and has been accepted for publication.

Accepted Manuscripts are published online shortly after acceptance, before technical editing, formatting and proof reading. Using this free service, authors can make their results available to the community, in citable form, before we publish the edited article. We will replace this *Accepted Manuscript* with the edited and formatted *Advance Article* as soon as it is available.

You can find more information about *Accepted Manuscripts* in the [Information for Authors](#).

Please note that technical editing may introduce minor changes to the text and/or graphics, which may alter content. The journal's standard [Terms & Conditions](#) and the [Ethical guidelines](#) still apply. In no event shall the Royal Society of Chemistry be held responsible for any errors or omissions in this *Accepted Manuscript* or any consequences arising from the use of any information it contains.

Efficient one-pot synthesis of Propargylamines catalysed by Gold nanocrystals Stabilized on montmorillonite

Bibek Jyoti Borah, Subrat Jyoti Borah, Kokil Saikia, Dipak Kumar Dutta*

Materials Science Division, CSIR-North East Institute of Science and Technology,
Jorhat, 785 006, Assam, India

*Corresponding Author: Tel: +91-376-2370 081, Fax: +91-376-2370 011.

E-mail: dipakkrdutta@yahoo.com

Abstract

The size selective Au⁰-nanoparticles were generated *in situ* into the nanopores of modified montmorillonite. The modification of montmorillonite was carried out with HCl under controlled conditions for generating nanopores (less than 8 nm) into the matrix and these nanopores act as “host” for *in situ* generation of Au⁰-nanoparticles. The synthesis consisted of impregnation of the acid-activated montmorillonite with HAuCl₄ aqueous solution followed by reduction with NaBH₄. The synthesised Au⁰-nanoparticles crystallized in the face centred cubic (fcc) lattice were single crystals with a preferential growth direction along the (111) plane. The N₂ adsorption/desorption study revealed specific surface areas (BET) of 327-579 m²/g, large specific pore volumes ~ 0.7 cm³/g, pore diameters 0-10 nm of the support. TEM, FESEM and X-ray studies indicate Au⁰-nanoparticles of 0-10 nm evenly distributed on the support and serve as an efficient green catalyst for one-pot, three-component (A³) coupling of an aldehyde, an amine and an alkyne *via* C-H alkyne-activation to synthesize propargylamines with 82-94% yield and 100% selectivity under mild reaction condition. The nanocatalysts can be recycled and reused several times without significant loss of their catalytic activity.

Keywords: Au⁰-nanoparticles; Montmorillonite; Face centred cubic; Propargylamines; C-H activation.

36 1. Introduction

37
38 The development of green chemistry is traced from the introduction of the concepts of
39 atom economy and utilization of non-hazardous metals in catalysis [1]. In this connection, a large
40 number of multicomponent reactions have been designed to synthesize different complex
41 molecules through a combination of three or more starting materials in one-pot condition [2].
42 Among the different multicomponent reactions, the catalytic coupling reaction of aldehyde,
43 amine and alkyne (so-called A³ coupling) is one of the best examples, where propargylamines is
44 produced as the main product [3]. Propargylamines have been attracting considerable attention
45 over the last few years due to their wide applications in drug discovery. Propargylamines are
46 versatile intermediates for the preparation of various nitrogen-containing compounds and are key
47 components of biologically active pharmaceuticals and natural products and also for the
48 synthesis of polyfunctional amino derivatives [4]. The importance of propargylamine motifs can
49 be best understood from the discovery of rasagiline, which contains propargylamine moiety
50 (trade name: Azilect), an FDA approved drug, that is prescribed for use as monotherapy in early
51 Parkinson's disease [4]. Various methods typically involve C-H bond activation of terminal
52 alkynes using a wide range of metals (e.g. Cu, Fe, Au, In, etc.) based catalysts have been well
53 explored for the synthesis of propargylamines [5].

54 In the recent years, there has been increasing interest in gold for using as catalysts in
55 organic transformations, though gold was traditionally considered to be chemically inert and
56 regarded as a poor catalyst. The development of nanometer sized gold particles is intensively
57 pursued because of their importance for both fundamental science and advanced technologies
58 [6]. The main reasons for extensive use of gold are that it exhibits some unusual and unexpected
59 properties in many organic transformations, highly stable in any form and more importantly the
60 non-toxic nature [7]. The gold based compounds are well-known to exhibit high alkynophilicity
61 for activating *sp* and even *sp*² and *sp*³ C-H bonds and this property has been exploited for making
62 it a promising catalyst in three-component A³ coupling reactions of terminal alkynes with
63 aldehydes and secondary amines [8]. In 2003, Li's group first reported the gold halides salts as a
64 catalyst for alkynylation of iminium ions [9]. Wong and co-workers have reported Au(III)salen
65 complex as a catalyst for A³ coupling reaction [10]. Although, these catalytic systems showed
66 good activity but the main disadvantages of these systems are that they are homogenous in nature

67 and are, therefore, not economically and environmentally attractive. During the last decade,
68 supported Au⁰-nanocatalytic systems are explored as sustainable and competitive alternative to
69 the gold complexes for A³ coupling reaction. Supported Au⁰-nanoparticles enhances the activity
70 and selectivity of the reaction and more importantly satisfied the stringent criteria of becoming
71 heterogeneous catalyst [2a,11]. In 2007, Kidwai and co-workers reported the first example of
72 gold nanocluster (16-20 nm) derived from the reduction of AuCl₃ by hydrazine as a catalyst for
73 the synthesis of propargylamine [11a]. Vinu and co-workers reported a new catalytic system for
74 A³ coupling reaction containing Au⁰-nanoparticles embedded in mesoporous carbon nitride,
75 however, they had restricted their experiments with only a few substrates [11c]. Kantam and co-
76 workers reported the nanocrystalline MgO stabilized Au⁰-nanoparticles based heterogeneous
77 catalyst for propargylamine synthesis [11b]. Very recently, Karimi's group successfully
78 synthesized Au⁰-nanoparticles supported on periodic mesoporous organosilica with ionic liquid
79 framework [2a]. Although, they have reported an efficient catalytic system for three-component
80 coupling reaction, but their support preparation process is laborious and time consuming.
81 Therefore, the development of new *greener*, efficient and recoverable Au-based catalytic system
82 for A³ coupling reaction is a challenge for researchers. Herein, we have reported a well-defined
83 heterogeneous catalytic system i.e. crystalline Au⁰-nanoparticles supported on modified
84 montmorillonite for one-pot synthesis of propargylamines. These nanoparticles maintain their
85 catalytic efficiency for several cycles and serve as potential reusable catalyst. The modified
86 montmorillonite is considered as environmentally benign, cheap, easily available and robust
87 support/stabilizer materials for the synthesis of different metal nanoparticles [12]. The virgin
88 montmorillonite is collected from the indigenous source i.e. natural deposits of western part of
89 India, which was purified and activated with mineral acid under controlled conditions to generate
90 a matrix having high surface area and contain micro- and mesopores with diameter in the range
91 0-10 nm. These nano range pores act as "host" for *in situ* generation of Au⁰-nanoparticles and
92 thus limit the growth of the particles upto desired range.

93
94
95
96
97

98 2. Experimental

99 2.1 Support preparation

100 Purified bentonite (10 g) was dispersed in 200 ml 4 M hydrochloric acid and refluxed for
101 various time intervals (1 and 2 h). After cooling, the supernatant liquid was discarded and the
102 activated montmorillonite was repeatedly redispersed in deionised water until no Cl^- ions could
103 be detected by the AgNO_3 test. The montmorillonite was recovered, dried in air oven at 50 ± 5
104 $^\circ\text{C}$ over night to obtain the solid product. These activated montmorillonites were designated as
105 AT-Mont.-I and AT-Mont.-II indicating the activation time of 1 and 2 h.

106 2.2 Au^0 -nanoparticles preparation

107 0.5 g of activated montmorillonite (AT-Mont.-I or -II) was impregnated by 15 ml (0.254
108 mmol) aqueous solution of HAuCl_4 under vigorous stirring condition. The stirring was continued
109 for another 5-6 h before the mixture was evaporated to dryness in a rotavapour. 0.3 g of the dry
110 composite was dispersed in 10 ml water and 134 mg NaBH_4 (3.54 mmol) in 10 ml distilled water
111 were added slowly over 15 min under constant stirring. The colour changed immediately from
112 yellow to dark violet. The mass was allowed to settle and washed with distilled water several
113 times until the content was free of Cl^- ions. The Au^0 -montmorillonite composite was collected
114 and dried at 60°C for 12 h and stored in airtight bottle. The samples thus prepared were
115 designated as Au^0 -Mont.-I and Au^0 -Mont.-II.

116 2.3 General procedure for the one-pot synthesis of propargylamines

117 Aldehyde (1 mmol), amine (1 mmol), alkyne (1.2 mmol), 20 mg catalyst (Au^0 -Mont.-I
118 or Au^0 -Mont.-II.) and 5 ml toluene were taken in a 25 ml round bottom flask and reaction
119 mixture was refluxed at 110°C for stipulated time period. The progress of the reactions was
120 monitored by TLC. After completion of the reaction, solid catalyst was separated from the
121 mixture by filtered through sintered funnel (G-3) and the solvent was removed under low
122 pressure in a rotavapour. The recovered catalyst was washed with acetone (30 ml), dried in a
123 desiccator and stored for another consecutive reaction run. The crude product obtained was then
124 purified by silica gel column chromatography using ethyl acetate and hexane as eluents. The
125 products were characterized by (^1H , ^{13}C) NMR and mass spectrometry and all gave satisfactory
126 results [supporting information].

127

128 3. Results and discussion

129 3.1. Characterization of Support

130 The naturally occurring montmorillonite is considered as cheap, easily available and
131 environmentally benign catalysts and catalyst supports [12a-f]. The raw virgin montmorillonite
132 was first purified by dispersion-cum-sedimentation technique and then treated with 4 M HCl and
133 refluxed for various time intervals (1 and 2 h) under controlled conditions in order to generate
134 high surface area and nanoporous matrix. The characterization of the modified montmorillonite
135 was thoroughly carried out with the help of different analytical instruments like Powder-XRD,
136 FT-IR, N₂ adsorption-desorption and SEM-EDX. The parent montmorillonite (Parent Mont.) is
137 2:1 layered dioctahedral aluminosilicate and consists of two tetrahedral silicate sheets which are
138 bonded to either side of an octahedral aluminate sheet having basal reflection at 7.06° 2θ
139 corresponding to a basal spacing of 12.5 Å. The powder XRD study reveals that, the intensity of
140 basal reflection decreased with increasing activation time and after 2 h acid activation i.e. in AT-
141 Mont.-II, the basal reflection is almost depleted which indicates that the layered structure of the
142 clay mineral is disrupted. During acid activation, the surface area (upto 578.5 m²/g) as well as
143 pore volume (~ 0.7 cm³/g) are increased in case of AT-Mont.-I (1 h treatment) due to the
144 leaching of Al from the octahedral sites, which also introduced micro- (< 2 nm) and mesopores
145 (> 2 nm) on the clay surface. The specific surface area of the clay matrix is decreased on
146 prolonging the acid activation time upto 2 h (AT-Mont.-II) because of destruction of the pore
147 walls without significantly changing the overall specific pore volume (Table 1). The pore size
148 increased with increasing the activation time because of the elimination of smaller pores and
149 formation of larger pores. The adsorption-desorption isotherms [Fig. 1] were of type-IV with a
150 H3 hysteresis loop at P/P₀ ~ 0.4-0.8, indicating mesoporous solids. The differential volumes
151 versus pore diameter plots i.e. BJH plot indicated relatively narrow pore size distributions with a
152 peak pore diameter 4.12 and 6.33 nm for AT-Mont.-I and AT-Mont.-II respectively and these
153 nano range pores were advantageously utilized for the *in situ* synthesis of various metal
154 nanoparticles as reported our group recently [12a-g]. The parent montmorillonite exhibited an
155 intense IR absorption band at ~1034 cm⁻¹ for Si-O stretching vibrations of tetrahedral sheet. The
156 bands at 522 and 460 cm⁻¹ were due to Si-O-Al and Si-O-Si bending vibrations. Upon acid
157 activation, the band ~1034 cm⁻¹ shifted to ~1083 cm⁻¹. The appearance of a pronounced band

158 near 800 cm^{-1} indicated amorphous silica. Montmorillonite also showed absorption bands at
159 3633 cm^{-1} due to stretching vibrations of OH groups of Al-OH. The bands at 917, 875 and 792
160 cm^{-1} were related to AlAl-OH, AlFe-OH and AlMg-OH vibrations. The gradual disappearance of
161 these bands during acid-activation indicated the removal of Al, Fe and Mg ions from the clay
162 mineral structure. The ^{29}Si and ^{27}Al MAS-NMR measurements and SEM-EDX studies also
163 confirmed that during acid activation, nano range pores are formed on the surface of clay matrix
164 due to Al leaching and predominant amounts of Si compared to Al were present on the surface
165 [12a-f] [supporting information].

166 3.2. Au⁰-nanoparticles characterization

167 The immediate evidence for the formation of Au⁰-nanoparticles was provided by UV-
168 visible spectroscopy. The appearance of surface plasmon resonance bands of different width at
169 around $\sim 520\text{ nm}$ of violet colour Au⁰-Mont.-I and Au⁰-Mont.-II substantiated its formation and
170 also suggested that maximum particle sizes are below 10 nm [Fig. 2]. Therefore, the nanopores
171 of clay matrix effectively controlled the size of the embedded Au⁰-nanoparticles and isolated
172 them from each other to avoid agglomeration.

173 The TEM images of nanoparticles composites showed that dispersed Au⁰-nanoparticles
174 were formed in the micro- and mesopores of AT-Mont.-I and AT-Mont.-II [supporting
175 information]. The supported Au⁰-nanoparticles were spherical in shape, well separated from each
176 other and with sizes of 0-10 nm. The distribution of the particles was dependent on the pore
177 diameter of the support. Some of the Au⁰-nanoparticles were found to be larger than the pore size
178 of the support. Typical HRTEM images of Au⁰-Mont.-I showed the reticular lattice planes inside
179 the nanoparticles [Fig. 3]. The lattice planes continuously extended to the whole particles
180 without stacking faults or twins, indicating the single crystalline nature. The measured
181 interplanar spacing for all lattice fringes was 2.35 \AA , which agrees with the (111) plane of fcc
182 gold crystals. The corresponding selected area electron diffraction (SAED) pattern of Au⁰-
183 nanoparticles obtained by focusing the electron beam on the nanoparticle lying flat on the TEM
184 grid is shown in Fig. 3 (inset). The formation of hexagonal symmetrical diffraction spot patterns
185 demonstrated that the Au⁰-nanoparticles are single crystals with a preferential growth direction
186 along the (111) plane.

187 The crystalline nature of the Au⁰-nanoparticles was also confirmed by the powder XRD
188 pattern [Fig. 4]. The four reflections were assigned to the (111), (200), (220) and (311)
189 diffraction of a fcc lattice of gold. The intensity ratio of the (200) and (111) reflections was
190 unusually lower than the conventional values (JCPDS file, 0.12 versus 0.33). These observations
191 confirmed that the synthesised Au⁰-nanoparticles were primarily dominated by (111) facets and
192 thus their (111) planes tend to be preferentially oriented parallel to the surface of the support
193 [13]. This result also substantiated the HRTEM and SAED observations.

194 The Au⁰-Mont.-I was analyzed by XPS in order to determine the electronic state of the
195 atom. The typical spectrum shows Au 4f doublet (4f_{5/2}, 88.3 eV and 4f_{7/2}, 84.6 eV) and peak-to-
196 peak distance (3.7 eV) [Fig. 5] which is in good agreement with the value due to Au(0) oxidation
197 state [14]. This indicates that the alumino-silicate constituent of clay matrix efficiently stabilized
198 Au⁰-nanoparticles in their well developed nanopores and prevents from oxidation during the
199 synthesis and stabilizing process.

200 The encapsulation of Au⁰-nanoparticles into the nanopores of the modified clay has
201 changed some of the textural parameters of the materials as observed from the Fig. 1 that Au⁰-
202 Mont.-I and Au⁰-Mont.-II exhibit similar type of isotherms and hysteresis loop with that of AT-
203 Mont. This reveals that the highly ordered porous structure of clay is still maintained even after
204 the encapsulation of Au⁰-nanoparticles. The appreciable decrease of the specific surface area and
205 the specific pore volume after supporting Au⁰-nanoparticles (Table 1) might be due to clogging
206 of some pores by Au⁰-nanoparticles. In addition, the presence of Au⁰-nanoparticles may
207 influence the adsorption measurements. However, increase of pore diameter may be due to
208 rupture of some smaller pores to generate bigger ones during the formation of Au⁰-nanoparticles
209 into the pores.

210 The Au contents in Au⁰-Mont.-I and Au⁰-Mont.-II as analyzed by ICP-AES, reveals the
211 presence of 0.048 mol % of Au in each catalyst.

212

213

214

215

216 3.3. Catalytic activity

217 In order to determine the best reaction condition (i.e. solvent, reaction time, etc.) that are
218 essential for the synthesis of propargylamines in an efficient way by our catalytic system, a series
219 of three-component coupling reactions were carried out using benzaldehyde, piperidine and
220 phenylacetylene as the model substrates in presence of Au⁰-Mont.-I as catalyst. In the solvent
221 screening study, initially different polar solvents like water, ethanol, methanol, acetonitrile were
222 used for the reaction, but no encouraging results were obtained and in case of THF, DMF
223 solvents, no products are formed even after 24 h of reaction time. Aromatic non-polar solvent
224 such as toluene, surprisingly, yielded 94% of desired propargylamine product. The reaction
225 required maximum 3 h for completion (as monitored by TLC) at the refluxing temperature of
226 toluene. Therefore, it is found that, the present catalytic systems (Au⁰-Mont.-I and Au⁰-Mont.-II)
227 proceed well in toluene at refluxing temperature. To understand the role of Au⁰-nanoparticles,
228 the model reaction was carried out in the optimized reaction condition using acid activated clays
229 (AT-Mont.-I or AT-Mont.-II) alone as catalyst and only 5-10% yield of the product was formed
230 (Table 2). A preliminary investigation was also carried out for the use of primary amines in the
231 reaction, but no encouraging results were found and hence only secondary amines were used in
232 the present study. Using optimized reaction conditions, we explored the versatility and
233 limitations of various substrates as well as efficiency of our catalysts for the said one-pot three-
234 components coupling reaction to synthesise propargylamines and the results are summarized in
235 Table 2. In this study, we used phenylacetylene, 3-butyne-1-ol and 1,6-heptadiyne as alkynes,
236 various electronically diverse aldehydes (e.g. benzaldehyde, 4-methoxybenzaldehyde, 4-
237 chlorobenzaldehyde etc.) and secondary amines (e.g. piperidine, morpholine, diethylamine) and
238 all the substrates produce the desired propargylamines with very good to excellent yields and
239 about 100% selectivity irrespective of nature of the substrates. The model reaction, i.e. coupling
240 between benzaldehyde, phenylacetylene and piperidine gives maximum 94% isolated yield when
241 Au⁰-Mont.-I is used as catalyst (entry 1). It is observed that the aromatic aldehydes containing
242 electron withdrawing group gave slightly higher yield than that bearing electron donating group.
243 The aliphatic alkyne i.e. 3-butyne-1-ol was allowed to react with two different iminium ions
244 generated *in situ* from benzaldehyde and piperidine (entry 9) and benzaldehyde and morpholine
245 (entry 10), it is found that desired propargylamines were formed with high yield. Again, the

246 aliphatic amine i.e. diethylamine (entry 7) showed lower conversion than the cyclic amine i.e.
247 piperidine and morpholine (entry 1 and entry 8). It is observed that, the catalyst, Au⁰-Mont.-I
248 showed slightly higher activity than Au⁰-Mont.-II. Therefore, Au⁰-Mont.-I was exclusively used
249 as catalyst for study with more substrates tolerance of the catalyst. Next, we explored our
250 strategy for the synthesis of symmetrical bis-propargylamines derivatives by coupling of
251 dialkyne, viz. 1,6-heptadiyne with benzaldehyde and piperidine (entry 11) and 4-
252 methoxybenzaldehyde and diethyl amine (entry 12), as expected, the desired products were
253 formed with good isolated yield (max. 85%) but the reactions needed a comparatively longer
254 time i.e. 5 h for completion. We have also used aliphatic aldehyde i.e. pentanal (entry 13) and
255 sterically hindered aldehyde i.e. 4-hydroxy-3-methoxybenzaldehyde (entry 14), the
256 corresponding propargylamines are formed with good isolated yield and selectivity.

257 The slightly higher conversion shown by catalyst Au⁰-Mont.-I over Au⁰-Mont.-II may be
258 due to their higher surface area in the former catalyst (Table 1). The pore volume and pore size
259 of the catalysts Au⁰-Mont.-I and Au⁰-Mont.-II, are adequate to carry out liquid phase catalytic
260 reactions (Table 1). Each catalyst was recovered by simple filtration technique after experiment.
261 The recovered catalyst was washed with acetone, dried in a desiccator and reused directly with
262 fresh reaction mixture without further purification for the desired coupling products synthesis
263 upto 3rd run. The results (Table 2, entries 15 and 16) showed that in each case, the catalyst
264 remain active for several run without significantly loss in efficiency. All the reactions were
265 carried out with 0.048 mol% of Au in Au⁰-Mont.-I and Au⁰-Mont.-II catalysts (Table 2).

266 The recovered catalyst was further investigated through N₂ adsorption-desorption and
267 HRTEM analysis. The identical shape of the isotherms and the hysteresis loop reveal that the
268 characteristics of the catalysts are retained even after successive reactions. The specific surface
269 areas of the recovered catalysts decrease compared to freshly prepared catalyst (Table 1). The
270 decrease of surface area of the recovered catalysts after each reaction may be due to the blockage
271 of pores by the reactant molecules. In the HRTEM analysis of recovered Au⁰-Mont.-I (after 3rd
272 run), it is found that a few particles aggregate, but the sizes are still below 10 nm [supporting
273 information]. These experimental results clearly suggest that the reactions undergo in a
274 heterogeneous process as well as the robustness character of the catalyst.

275 A probable reaction mechanism for the one-pot, three components coupling of propargyl-
276 amines catalyzed by Au⁰-Mont.-I or Au⁰-Mont.-II under heterogeneous conditions is proposed.
277 The proposed mechanism is pictorially illustrated in Scheme 1. In the first step, Au⁰-
278 nanoparticles supported on AT-Mont. activate the C–H bond of the terminal alkyne to generate a
279 gold-alkylidene complex on the surface of the AT-Mont. This is a very favourable step because
280 Au⁰ is well known to exhibit high alkynophilicity for terminal alkynes [6]. The second step
281 involves the reaction between the gold-alkylidene complex formed, and the iminium ion which is
282 generated *in situ* from the reaction between aldehyde and secondary amine, to give the desired
283 product and the catalyst is regenerated. The theoretical by-product obtained from the reaction is
284 only water. The regenerated catalyst continues the catalytic cycles till the completion of the
285 reaction.

286 4. Conclusion

287 The nanoporous modified montmorillonite was found to be excellent eco-friendly support
288 for the *in situ* synthesis of Au⁰-nanoparticles with different sizes. The Au⁰-nanoparticles
289 crystallized in the *fcc* lattice were single crystals with a preferential growth direction along the
290 (111) plane. These nanoparticles demonstrated high catalytic activity in the one-pot three
291 components coupling of aldehydes, amines and alkynes *via* C-H activation for the synthesis of
292 propargylamine under mild reaction condition. Further, the nanocatalysts were reused for a new
293 batch of reactions without significant loss of their activity under the same conditions. The
294 operational simplicity and robustness of the catalyst, make it attractive not only for the large
295 scale synthesis of this class of biologically active molecules, but also for the exploration in the
296 synthesis of important drug intermediates.

Acknowledgements

The authors are grateful to Dr. D. Ramaiah, Director, CSIR-North East Institute of Science and Technology, Jorhat, Assam, India, for his kind permission to publish the work. The authors are also thankful to CSIR, New Delhi, for financial support (XIIth FYP Network project: BSC 0112, CSC 0125 and CSC 0135 and In-house Project: MLP-6000/01). The authors SJB and KS are grateful to UGC, New Delhi for providing research fellowship.

References

- [1] (a) R. A. Sheldon, *Chem. Commun.* 2008, 3352; (b) R. A. Sheldon, *Chem. Soc. Rev.* 2012, **41**, 1437.
- [2] (a) B. Karimi, M. Gholinejad, M. Khorasani, *Chem. Commun.* 2012, **48**, 8961; (b) M. Syamala, *Org. Prep. Proced. Int.* 2009, **41**, 1.
- [3] (a) G. Dyker, *Angew. Chem., Int. Ed.*, 1999, **38**, 1698; (b) J. Gao, Q.-W. Song, L.-N. He, Z.-Z. Yang, X.-Y. Dou, *Chem. Commun.*, 2012, **48**, 2024; (c) V. A. Peshkov, O. P. Pereshivko, E. V. V. Eycken, *Chem. Soc. Rev.* 2012, **41**, 3790; (d) W. J. Yoo, L. Zhao, C. J. Li, *Aldrichimica Acta* 2011, **44**, 43; (e) M. A. Huffman, N. Yasuda, A. E. Decamp, E. J. J. Grabowski, *J. Org. Chem.* 1995, **60**, 1590.
- [4] (a) M. Yogev-Falach, T. Amit, B.-O. Am, M. B. H. Youdim, *Faseb J.* 2003, **17**, 2325; (b) C. Binda, F. Hubalek, M. Li, Y. Herzig, J. Sterling, D. E. Edmondson, A. Mattevi, *J. Med. Chem.*, 2004, **47**, 1767; (c) D. A. Gallagher, A. Schrag, *CNS Drugs*, 2008, **22**, 563; (d) C. W. Olanow, *Neurology* 2006, **66**, S69-S79.
- [5] (a) B. Sreedhar, P. S. Reddy, B. V. Prakash, A. Ravindra, *Tetrahedron Lett.* 2005, **46**, 7019; (b) S. B. Park, H. Alper, *Chem. Commun.* 2005, 1315; (c) M. J. Albaladejo, F. Alonso, Y. Moglie, M. Yus, *Eur. J. Org. Chem.* 2012, 3093, (d) J. Gao, Q-W. Song, L-N. He, Z-Z. Yang, X-Y Dou, *Chem. Commun.* 2012, **48**, 2024; (e) T. Zeng, W-W. Chen, C. M. Cirtiu, A. Moores, G. Song, C-J. Li, *Green Chem.* 2010, **12**, 570; (f) X. Zhang, A. Corma, *Angew. Chem. Int. Ed.* 2008, **47**, 4358; (g) M. Rahman, A. K. Bagdi, A. Majee, A. Hajra, *Tetrahedron Lett.* 2011, **52**, 4437; (h) B. J. Borah, S. J. Borah, L. Saikia, D. K. Dutta, *Catal. Sci. & Technol.*; 2014, **4**, 1047.
- [6] (a) M. Haruta, *Chem. Rec.* 2003, **3**, 75; (b) E. Boisselier, D. Astruc, *Chem. Soc. Rev.* 2009, **38**, 1759; (c) G. J. Hutchings, M. Brust, H. Schmidbaur, *Chem. Soc. Rev.* 2008, **37**, 1759; (d) D. L. Feldheim and C. A. Foss, Jr (Eds.), *Metal Nanoparticles: Synthesis*,

- Characterization and Application*, CRC Press, New York (2002); (e) J. M. Campelo, D. Luna, R. Luque, J. M. Marinas, A. A. Romero, *ChemSusChem* 2009, **2**, 18; (f) B. C. Ranu, K. Chattopadhyay, L. Adak, A. Saha, S. Bhadra, R. Dey, D. Saha, *Pure and Appl. Chem.* 2009, **81**, 2337.
- [7] H. Qian, L. A. Pretzer, J. C. Velazquez, Z. Zhao, M. S. Wong, *J Chem Technol Biotechnol* 2013, **88**, 735.
- [8] (a) C. Wei, C.-J. Li, *J. Am. Chem. Soc.*, 2003, **125**, 9584; (b) B. Huang, X. Yao, C. -J. Li, *Adv. Synth. Catal.*, 2006, **348**, 1528; (c) V. K.-Y. Lo, Y. Liu, M.-K. Wong, C. -M. Che, *Org. Lett.*, 2006, **8**, 1529; (d) L. L. Chng, J. Yang, Y. Wei, J. Y. Ying, *Adv. Synth. Catal.*, 2009, **351**, 2887; (e) X. Zhang, A. Corma, *Angew. Chem., Int. Ed.*, 2008, **47**, 4358.
- [9] (a) C. Wei, Z. Li, C. -J. Li, *Org. Lett.* 2003, **5**, 4473; (b) C. Wei, C. -J. Li, *J. Am. Chem. Soc.* 2003, **125**, 9584.
- [10] V. K. -Y. Lo, Y. Liu, M. -K. Wong, M. -K. Che, *Org. Lett.* 2006, **8**, 1529.
- [11] (a) M. Kidwai, V. Bansal, A. Kumar, S. Mozumdar, *Green Chem.* 2007, **9**, 742; (b) K. Layek, R. Chakravarti, M. Lakshmi Kantam, H. Maheswaran, A. Viru, *Green Chem.* 2011, **13**, 2878; (c) K. K. R. Datta, B. V. S. Reddy, K. Ariga, A. Vinu, *Angew. Chem., Int. Ed.*, 2010, **49**, 5961.
- [12] (a) B. J. Borah, D. Dutta, P. P. Saikia, N. C. Barua, D. K. Dutta, *Green Chem.* 2011, **13**, 3453; (b) B. J. Borah, D. K. Dutta, *J. Mol. Catal. A: Chem.* 2013, **366**, 202; (c) P. P. Sarmah, D. K. Dutta, *Green Chem.* 2012, **14**, 1086; (d) B. J. Borah, D. Dutta, D. K. Dutta, *Appl. Clay Sci.*, 2010, **49**, 317; (e) D. Dutta, B. J. Borah, L. Saikia, M. G. Pathak, P. Sengupta, D. K. Dutta, *Appl. Clay Sci.* 2011, **53**, 650; (f) L. Saikia, D. Dutta, D. K. Dutta, *Catal. Commun.* 2012, **19**, 1; (g) D. K. Dutta, D. Dutta, P. P. Sarmah, S. K. Bhorodwaj, B. J. Borah, *J. Biomed. Nanotechnol.* 2011, **7**, 76; (h) B. J. Borah, K. Saikia, P. P. Saikia, N. C. Barua, D. K. Dutta, *Catal. Today* 2012, **198**, 174.
- [13] (a) Y. Luo, *Mater. Lett.* 2006, **60**, 3361; (b) X. Sun, S. Dong, E. Wang, *Langmuir* 2005, **21**, 4710.
- [14] (a) P. M. Shem, R. Sardar and J. S. Shumaker-Perry, *Langmuir* 2009, **25**, 13279; (b) M. P. Casaletto, A. Longo, A. Martorana, A. Prestianni and A. M. Venezia, *Surf. Interface Anal.* 2006, **38**, 215.

Table 1: Surface properties of montmorillonite based supports/catalysts

Samples	Surface properties			
	Specific surface area (m ² /g)	Average Pore diameter (nm)	Specific pore volume (cm ³ /g)	
AT-Mont.-I	578.5	4.12	0.596	
AT-Mont.-II	400.5	6.33	0.604	
Au ⁰ -Mont.-I	Fresh	305.3	5.31	0.285
	After 1 st run	265.6	6.12	0.253
	After 2 nd run	230.5	7.44	0.231
	After 3 rd run	210.3	8.01	0.206
Au ⁰ -Mont.-II	Fresh	265.3	7.66	0.368
	After 1 st run	234.8	8.22	0.315
	After 2 nd run	216.3	9.01	0.277
	After 3 rd run	201.2	9.23	0.249

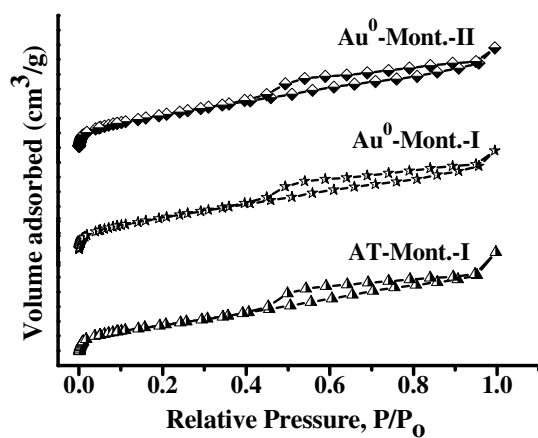


Fig. 1. N₂ adsorption-desorption isotherms of support and catalysts.

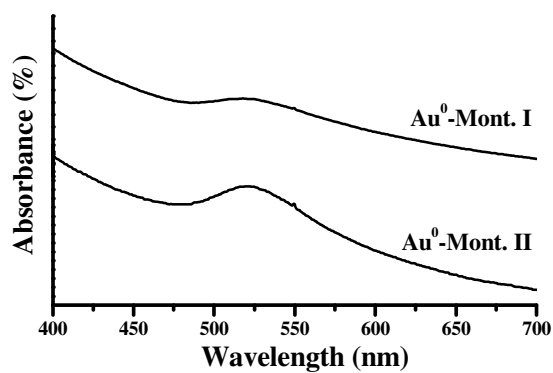


Fig. 2. UV-Visible spectra of Au⁰-Mont.-I and Au⁰-Mont.-II.

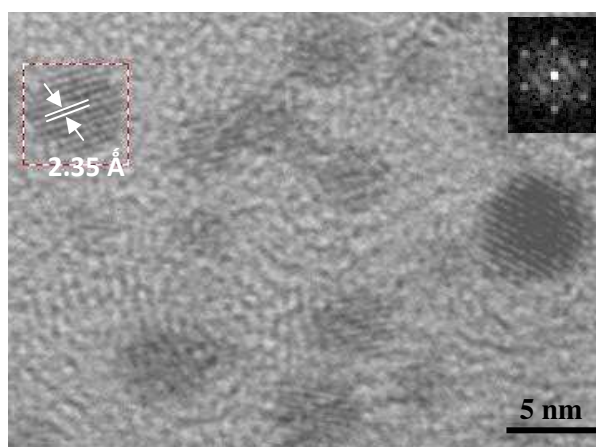


Fig. 3. HRTEM image and corresponding SAED pattern (inset) of Au⁰-Mont.-I.

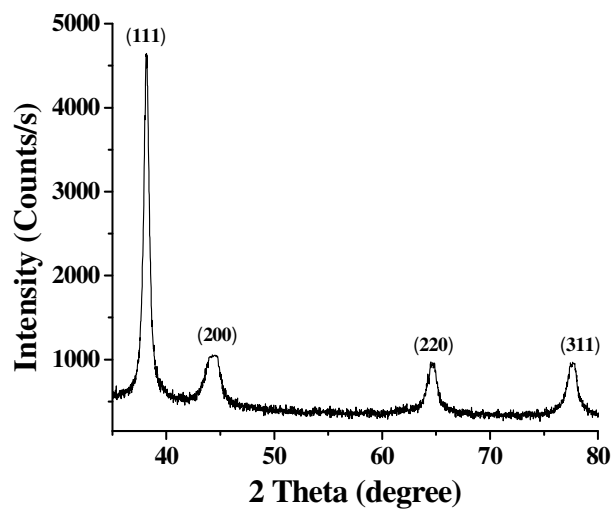


Fig. 4: Powder XRD pattern of Au⁰-nanoparticles (Au⁰-Mont.-I).

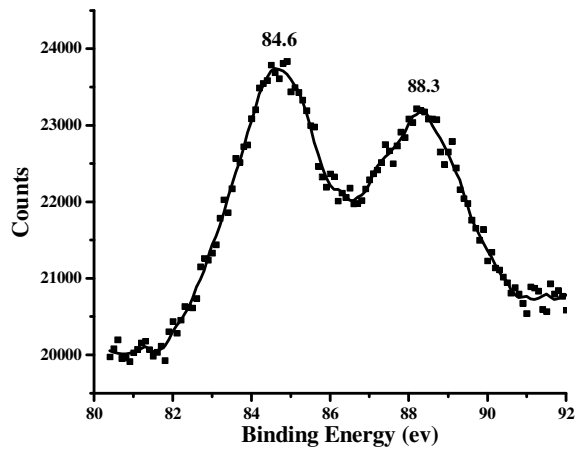
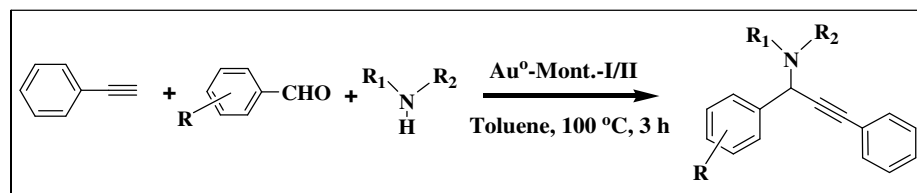
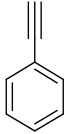
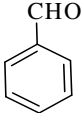
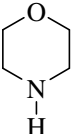
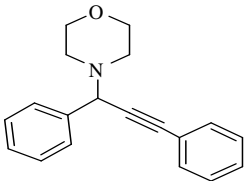
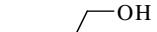
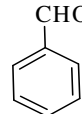
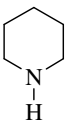
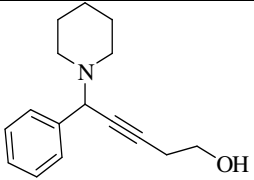
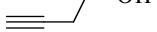
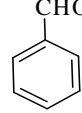
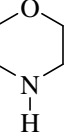
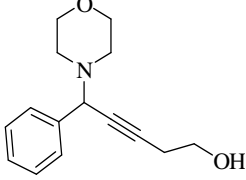
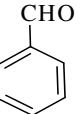
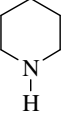
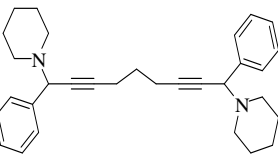
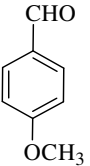
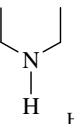
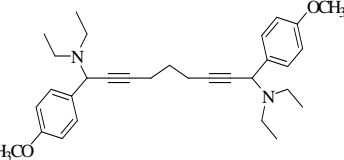
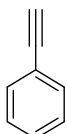
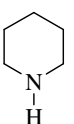
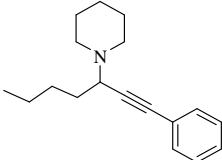
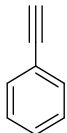
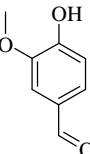
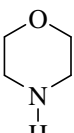
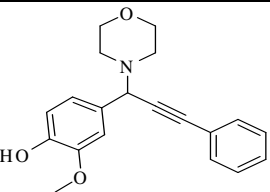
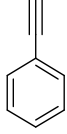
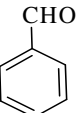
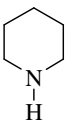
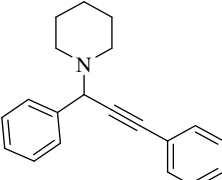


Fig. 5. XPS spectrum of Au⁰-Mont.-I.

Table 2. Three-component coupling of aldehyde, alkyne and amine for the synthesis of propargylamine.

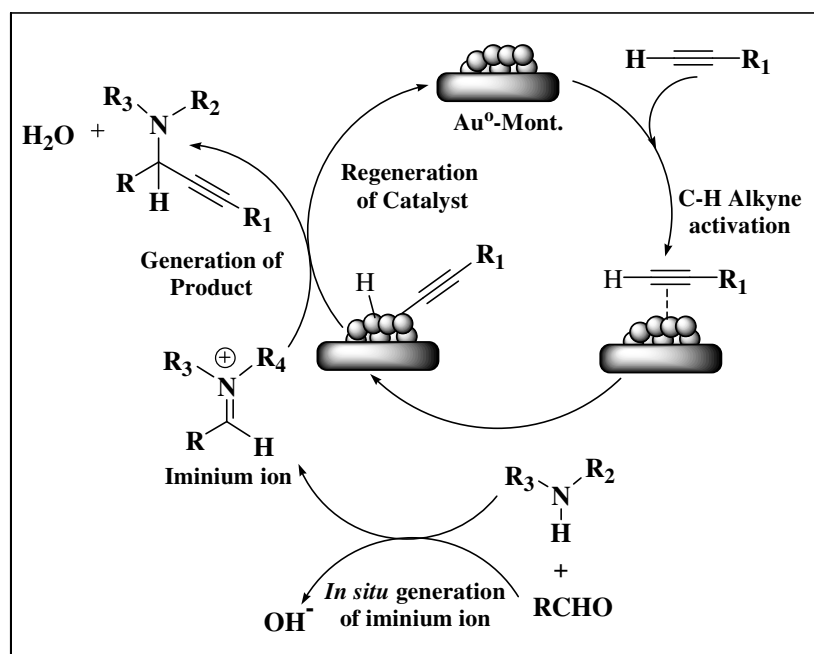
Entry	Alkyne	Aldehyde	Amine	Products	Catalyst	Yield* (%)
1					Au ⁰ -Mont.-I	94
					Au ⁰ -Mont.-II	91
2					Au ⁰ -Mont.-I	88
					Au ⁰ -Mont.-II	85
3					Au ⁰ -Mont.-I	86
					Au ⁰ -Mont.-II	84
4					Au ⁰ -Mont.-I	89
					Au ⁰ -Mont.-II	85
5					Au ⁰ -Mont.-I	86
					Au ⁰ -Mont.-II	82
6					Au ⁰ -Mont.-I	91
					Au ⁰ -Mont.-II	88
7					Au ⁰ -Mont.-I	86
					Au ⁰ -Mont.-II	83

8					Au ⁰ -Mont.-I	91
					Au ⁰ -Mont.-II	88
9					Au ⁰ -Mont.-I	86
					Au ⁰ -Mont.-II	82
10					Au ⁰ -Mont.-I	84
11					Au ⁰ -Mont.-I	85**
12					Au ⁰ -Mont.-I	83**
13					Au ⁰ -Mont.-I	88
14					Au ⁰ -Mont.-I	83
15					Au ⁰ -Mont.-I (2 nd run)	91
					Au ⁰ -Mont.-I (3 rd run)	88

16		Au ⁰ -Mont.-II (2 nd run)	85
		Au ⁰ -Mont.-II (3 rd run)	82
17		AT-Mont.-I	10
		AT-Mont.-II	5

***Yields** are isolated products based on benzaldehyde after silica-gel column chromatography,
Reaction conditions: Aldehyde (1 mmol), Amine (1 mmol), Alkyne (1.2 mmol), Catalyst (20 mg, contain 0.0084 mmol Au) and Toluene (5 ml); Refluxing temp. 100 °C, Time 3 h.

**Time required for completion of reactions is 5 h.



Scheme 1: Tentative reaction mechanism of A³ coupling reaction

Efficient one-pot synthesis of Propargylamines catalysed by Gold nanocrystals Stabilized on montmorillonite

Bibek Jyoti Borah, Subrat Jyoti Borah, Kokil Saikia and Dipak Kumar Dutta*

Materials Science Division, CSIR-North East Institute of Science and Technology, Jorhat 785006, Assam, India, Fax: (+) 91 376 2370011, *E-mail: dipakkrdutta@yahoo.com

Graphical Abstract

The size selective Au⁰-nanoparticles were generated *in situ* into the nanopores of environmentally benign modified montmorillonite and their catalytic performance in three components (A³) coupling reactions of Aldehyde, Amine and Alkyne in one-pot to synthesize propargylamines with excellent yield and selectivity.

